Chapter 2

Experimental Methods

This chapter discusses the basic methods used to characterize the materials in this study with the exception of Seebeck coefficient metrology, which is described in detail in Chapter 3.

2.1 Transport Measurements

Thermoelectric materials are characterized by the figure-of-merit zT. In the introduction I discussed the thermodynamic meaning of zT. However, that is only one half of its utility. The other half is that it is composed of material properties which are readily measured. We have:

$$zT = \frac{\sigma\alpha^2}{\kappa}T \tag{2.1}$$

In this work κ was not measured directly. Instead the thermal conductivity is expressed as:

$$\kappa = \rho D_t c_p \tag{2.2}$$

And each component of Equation 2.2 is measured separately. To obtain zT six quantities must be measured: ρ, D_T, α, σ, c_p, and T. Additionally, for characterization of the band structure properties the Hall coefficient (R_H) is measured. From R_H and σ it is possible to determine the Hall carrier concentration (n_H) and the Hall mobility (μ_H). These quantities are macroscopic measurements of the band structure and can be used to determine its form.

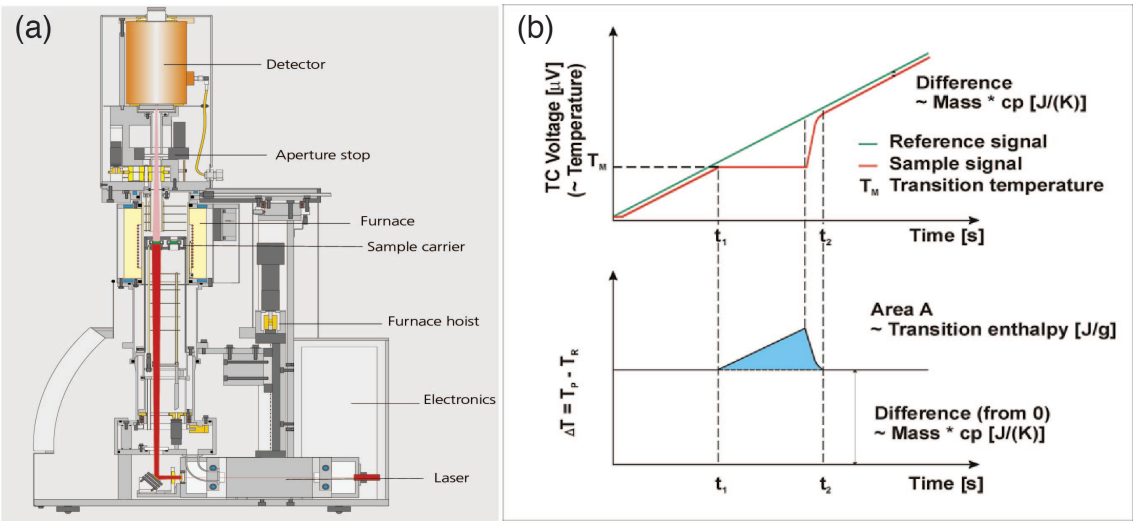

Figure 2.1: Schematic (a) of laser flash apparatus (LFA) and graphical representation of differential scanning calorimetry. (DSC) Image credit to Netzch Corporation.

Thermal diffusivity (D_T) was measured via the laser flash method. In this method a laser is pulsed upon the sample quickly, and the temperature on the other side is measured as a function of time. By fitting the temperature rise data a thermal diffusivity can be obtained. The timescale of the laser pulse must be much smaller than the rise time. The measurements presented in this thesis were measured using a Netzsch LFA (Laser Flash Analysis) 457 MicroFlash apparatus, see Figure 2.1.

The density (ρ) was measured by direct geometry. Measured samples typically have a regular geometry — either a rectangular prism or a cylinder. By measuring these regular dimensions with a pair of calipers or a micrometer the volume can be calculated. The sample mass is then measured on a calibrated scale. From measured mass and volume the geometric density is calculated.

Differential scanning calorimetry was used to obtain the specific heat capacity using a Netzsch DSC 404. In the case of Cu_2Se the measurements were confirmed using a Quantum Design PPMS. The measurements are courtesy of Huili Liu and Xun Shi of the Shanghai Institute of Ceramics at the Chinese Academy of Sciences (SIC-CAS) and also of Pawan Gogna of the JPL Thermoelectrics Group. The working principle of DSC is to increase the temperature of a heat bath in contact with both a sample and a reference at a constant rate. Due to the fixed rate of heat transfer there

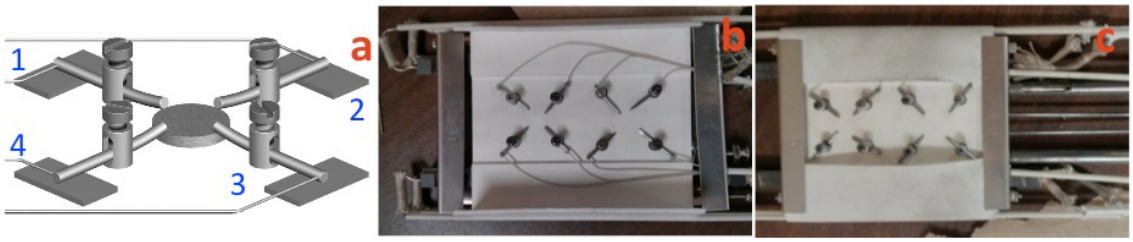

Figure 2.2: Resistivity and Hall coefficient were measured by the four point Van der Pauw method. Image courtesy of Heng Wang.

will be a lag in the measured temperature of a sample that is proportional to its heat capacity, see Figure 2.1. The PPMS c_p measurement is similar except quasi-static. The sample is brought to a stable temperature and then a reservoir temperature pulse is applied while the sample temperature deviation is measured.

Two Van der Pauw geometry resistivity systems were used in this study to obtain σ, n_H and μ_H. Both systems are of identical design. A system with a 1 T magnet at the JPL thermoelectrics group was used to obtain the Hall data for Cu_2Se; all other data was obtained with a 2 T system at Caltech. The design and function of these particular systems is described in a recent publication by Borup *et al.* [20].

The Hall coefficient is measured by applying a magnetic field, measuring the voltage, and applying a current in three orthogonal directions. In Figure 2.2 the mangetic field would be applied through the sample, while the current is applied from lead 1 to lead 3 and voltage measured from lead 2 to 4. The current direction and leads used were alternated in accordance with the Van der Pauw resistivity method. The measurement were made at both positive and negative applied field to eliminate magnetoresistive offsets. In the case of a single carrier the Hall resistance is related to the carrier concentration by [160]:

$$R_H = \frac{1}{nq} \tag{2.3}$$

If there are carriers of multiple type their contribution to the Hall resistance will depend on the applied field (B) as detailed in Jaworski *et al.* [92] and a recent publication I authored [25]. Though the full expansion is extremely complicated, for

either the limit of $B \gg \mu^{-1}$ or $B \ll \mu^{-1}$ the form is much simpler. This condition corresponds to whether the carrier velocity is primarily due to electron drift (small B) or cyclotron acceleration (large B). The high field limit is:

$$R_H = \frac{1}{n_1 q_1 + n_2 q_2} \tag{2.4}$$

While the low field limit is:

$$R_H = \frac{n_1 \mu_1^2 + n_2 \mu_2^2}{(n_1 q_1 \mu_1 + n_2 q_2 \mu_2)^2} \tag{2.5}$$

In the low-B limit R_H is dependent on the square of carrier mobility, while in the high-B limit it only depends linearly on band mobility. Therefore if there is a high mobility minority carrier and a low mobility majority carrier, the minority carrier will dominate the behavior at low-B while the majority carrier dominates at high-B.

Sample	α	σ	D_T	C_p
Ag_2Se	0	15	15	0
Cu_2Se	0	10	5	0
$Cu_{1.97}Ag_{0.03}Se$	0	15	15	0

Table 2.1: Temperature Shifts for Transport Properties

The instruments described in this chapter are designed for typical thermoelectric samples in which transport properties have slowly varying temperature dependences. A temperature misreading of 10 K or 20 K will have no noticeable effect on the progression of zT in such materials. Near the phase transition it can lead to crucial misinterpretation of the results.

The abruptness of the phase transition allows a ready means of determing the actual offsets. The temperatue of the phase transition in Seebeck was taken as the phase transition temperture. In a Seebeck measurement care is taken in instrument design to ensure that the temperature measured is that of the sample. Two thermocouples are used, which allows determination of thermocouple failure through comparison. Finally the Seebeck measurement is path independent [49] — the voltage only depends on the temperatures at the meaurement points without regard for temperature

irregularities in the sample. This contrasts to the volumetric measurements of D_T, c_p, and σ.

The temperature peak of heat capacity agreed with where the transition temperature determined by Seebeck measurement. The temperature offset in thermal diffusivity was due to misplacement of the measurement thermocouple. By moving the thermocouple into position the error could be reduced substantially. An encapsulated sample of Indium was measured during thermal diffusivity and the difference between its observed temperature of melting and its literature value (156.6 °C) was used to confirm the calibration. Electrical conductivity could not be checked the same way, and its calibration could not be confirmed. The values of these calibrations are in table 2.1.

2.2 Synthesis

The samples measured for this thesis were synthesized by Tristan Day at Caltech. A more detailed report on their synthesis will be available in his Ph.D. thesis (expected publication 2015). Ingots of Cu_2Se and $Cu_{1.97}Ag_{0.03}Se$ were prepared from mixtures of copper shot (Alfa Aesar, Puratronic, 99.999% pure on a metals basis), silver shot (Alfa Aesar, Puratronic, 99.999% pure on a metals basis), and selenium shot (Alfa Aesar, Puratronic, 99.999% pure on a metals basis) in stoichiometric ratios. The mixtures were placed in carbon-coated quartz ampoules evacuated to a pressure of less than 5×10^{-5} torr. The ampoules were heated to 1273 K at 100 K/hr and held at that temperature for five days. The ampoules were cooled to 973 K and annealed for three days, after which the ampoules were quenched in water. The ingots were then ball-milled. The resulting powder was hot-pressed [116] at 40 MPa and 923 K for five hours under argon flow. The pressed pellets were then cooled to room temperature at a rate of 5 K/min to avoid cracking.

Ag_2Se polycrystalline ingots were prepared by melting Ag (shot, 99.9999% pure, Alfa Aesar, Puratronic) and Se (shot, 99.999% pure, Alfa Aesar, Puratronic) in the desired mass ratios inside fused quartz ampoules evacuated to less than $6 \times 10^{-5} torr$.

The elements were slowly brought to 1273 K, held at that temperature for 12 hours, cooled to 973 K over three hours, annealed at 973 K for three days, then quenched in water. Disk-shaped samples were cut from the ingots and used directly for the experiments.

2.3 Chemical Characterization

X-ray diffractometry was performed with the assistance of Kasper Borup, Sebastian Christensen, and Bo B. Iversen of Aarhus University. PXRD was performed using a Rigaku SmartLab diffractometer configured with a Cu Kα source and a Rigaku D/tex detector. Temperature were performed using the same system and an Anton-Paar DHS-1100 furnace. The FullProf software suite was used for the refinements. X-ray diffraction allowed confirmation of composition by crystallography. Temperature resolved crystallography was used to determine the nature of the phase transition.

The Pair Distribution Function (p.d.f.) derived from total scattering measurements was performed on Cu_2Se to further elucidate the nature of the phase transition. The data was collected at beamline 11-ID-B, APS and analyzed by Sebastian Christensen. The utilized wavelength was $\lambda = 0.2128\,\text{Å}$ giving a $Q_{max} = 26\,\text{Å}^{-1}$. Samples were packed in 1.1 mm glass capillary within a glove box and sealed using epoxy glue. A dataset was obtained for every ≈5 K. Data collection time per dataset was 1 minute. Data was collected at equivalent temperatures on an empty capillary for background subtraction. Data was integrated using Fit2D. All datasets needed to be normalized to the incoming intensity because the ring was in decay mode during the experiment. The reduced pair distribution function, $g(r)$ was calculated by PDFgetX3. For the calculation we chose: $q_{min} = 0.8\,\text{Å}^{-1}$ and $q_{max} = 26\,\text{Å}^{-1}$.

Secondary measurements were performed via scanning electron microscopy (SEM) and electron probe microanalysis (EPMA). Wavelength dispersive spectroscopy (WDS) and energy dispersive spectroscopy (EDS) were performed respectively during EPMA and SEM. SEM (ZEISS 1550 VP) and EDS of Ag_2Se and Cu_2Se indicated them to be phase pure. EPMA and WDS were performed by Tristan Day with assistance from

Figure 2.3: Electron micrographs of $Cu_{1.97}Ag_{0.03}Se$ (a) and Cu_2Se (b). Black features are cavities. While Cu_2Se is single phase, $Cu_{1.97}Ag_{0.03}Se$ has inclusions of a silver rich phase (white) identified as CuAgSe by crystallography.

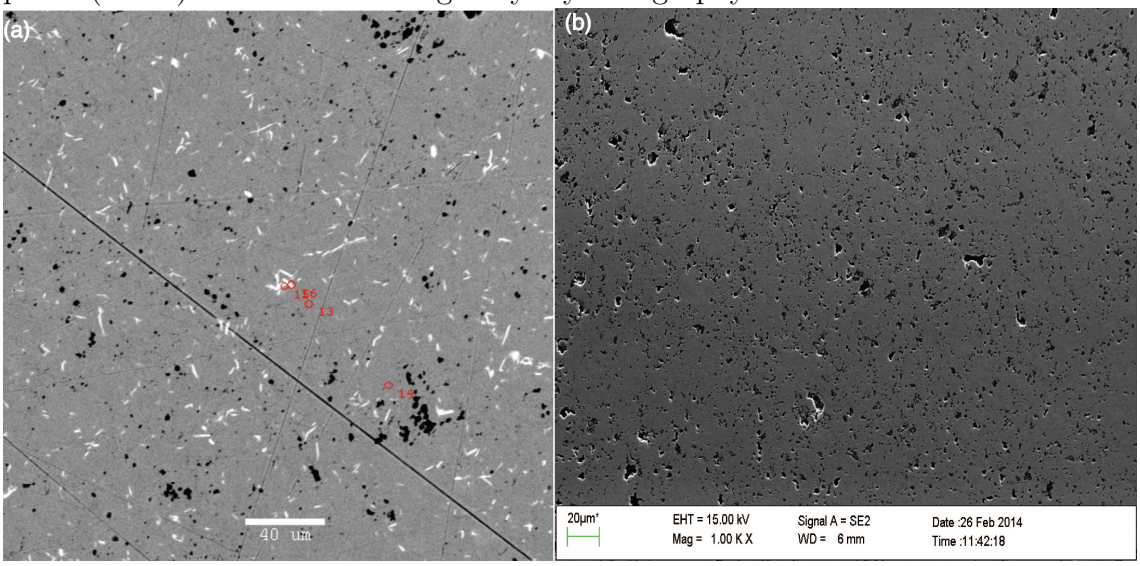

Dr. Chi Ma using a JEOL JXA-8200. WDS is considered to be more accurate than EDS and this advantage is amplified by the careful calibration to standards of the WDS detector. WDS on Cu_2Se confirmed the sample to be stoichiometric within the uncertainty of the measurement (0.5%). However, SEM of Cu_2Se indicated the presence of small cavities along the surface, see Figure 2.3(b). These cavities have been observed previously and identified as being from cavitation of Cu_2O and Se_2O_3 from trace oxygen in the material [101]. Any such oxygen secondary phase is undetectable by WDS due to the surface morphology and was also below the quantity for detection in any of the many X-ray measurements done during my studies. $Cu_{1.97}Ag_{0.03}$ shows a secondary silver rich phase that is identified as CuAgSe, see Figure 2.3(a).